

Efficient and Long-Living Light-Emitting Electrochemical Cells

By Rubén D. Costa, Enrique Ortí, Henk J. Bolink,* Stefan Graber, Catherine E. Housecroft, and Edwin C. Constable*

Three new heteroleptic iridium complexes that combine two approaches, one leading to a high stability and the other yielding a high luminescence efficiency, are presented. All complexes contain a phenyl group at the 6-position of the neutral bpy ligand, which holds an additional, increasingly bulky substituent on the 4-position. The phenyl group allows for intramolecular π - π stacking, which renders the complex more stable and yields long-living light-emitting electrochemical cells (LECs). The additional substituent increases the intersite distance between the cations in the film, reducing the quenching of the excitons, and should improve the efficiency of the LECs. Density functional theory calculations indicate that the three complexes have the desired π - π intramolecular interactions between the pendant phenyl ring of the bpy ligand and the phenyl ring of one of the ppy ligands in the ground and the excited states. The photoluminescence quantum efficiency of concentrated films of the complexes improves with the increasing size of the bulky groups indicating that the adopted strategy for improving the efficiency is successful. Indeed, LEC devices employing these complexes as the primary active component show shorter turn-on times, higher efficiencies and luminances, and, surprisingly, also demonstrate longer device stabilities.

1. Introduction

Solid-state light-emitting electrochemical cells (LECs) have attracted considerable interest in the past few years.^[1] LECs are single-component electroluminescent devices consisting of a charged luminescent material.^[1,2] The main characteristic of these

devices is the insensitivity to the work-function of the electrodes employed. This is due to the generation of a strong interfacial electric field caused by the displacement of the mobile ionic species towards the electrodes when an external electric field is applied over the device. The interfacial fields at the electrodes screen the electric field in the bulk material, which implies that the layer thickness of the emitting material is not very critical and in turn leads to fault-tolerant device architectures.^[3-6] Hence, in contrast to organic light-emitting diodes (OLEDs), devices with simple architecture and air-stable electrodes such as gold, silver, or aluminum can be fabricated, which is an initial requirement for obtaining unencapsulated devices.

In its simplest form, a LEC consists of a single active layer composed entirely of an ionic transition metal complex (iTMC) balanced by small mobile counteranions such as PF_6^- or BF_4^- . In iTMC-based LECs, the ionic complexes perform all the necessary roles for the generation of light: a) the

lowering of the injection barrier by the displacement of the counterions, b) the transport of electrons and holes by consecutive reduction and oxidation, respectively, of the iTMC, and c) the generation of photons by phosphorescence. iTMCs are triplet emitters similar to those used in OLEDs and, as expected, high efficiencies have been reported.^[7-10] Furthermore, as they are ionic, the iTMCs dissolve in polar, environmentally friendly solvents and are easily processed in thin films. iTMC-based LECs exhibiting low turn-on times and emitting blue, green, orange, red, and even white light have been reported although device lifetimes are generally low.^[11-18] Recently, we reported on a new approach to iTMCs that led to a significant increase in the stability of LECs that employed them as the main component.^[19-21] This was achieved with iridium complexes exhibiting intramolecular π - π stacking interactions between pendant phenyl groups and coordinated ligands, resulting in a supramolecular cage formation in the ground and the excited states. The simplest example is mentioned in this work for comparison and is referred to as complex 1 (Fig. 1).

To date, no device involving a single complex has exhibited low turn-on times, high efficiency, and high stability. It is the object of this present work to combine in one single complex features leading to a high stability and to a high luminescence efficiency.

[*] Dr. H. J. Bolink, R. D. Costa, Prof. E. Ortí
Instituto de Ciencia Molecular
Universidad de Valencia
PO Box 22085, Valencia (Spain)
E-mail: henk.bolink@uv.es

Dr. H. J. Bolink
Fundació General de la Universitat de Valencia (FGUV)
PO Box 22085, Valencia (Spain)

Prof. E. C. Constable, Dr. S. Graber, Prof. C. E. Housecroft
Department of Chemistry
University of Basel
Spitalstrasse 51, Basel, CH-4056 (Switzerland)
E-mail: edwin.constable@unibas.ch

DOI: 10.1002/adfm.201000043

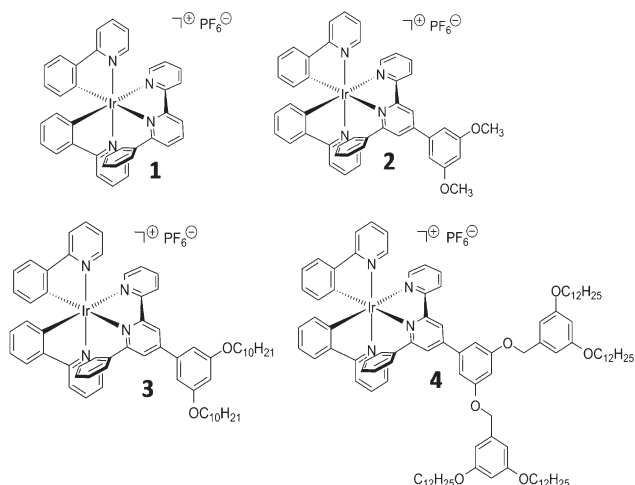


Figure 1. Chemical structures of the new complexes **2**, **3**, and **4**, and of reference compound **1**.

The external quantum efficiency (EQE) is defined as

$$\text{EQE} = b\varphi/2n^2 \quad (1)$$

where b is the recombination efficiency (equal to 1 for two ohmic contacts^[22]), φ is the fraction of excitons that decay radiatively, and n is the refractive index of the glass substrate and is equal to 1.5 (the factor $1/2n^2$ accounts for the coupling of light out of the device). As Ir(III)-based complexes can efficiently harvest both singlet and triplet excitons, φ should resemble the photoluminescence (PL) efficiency. Hence, the efficiency of the device is mainly determined by the PL quantum efficiency (PLQE) of the iTMC emitter in a solid film. Therefore, high device efficiencies can be reached when the quenching of excitons is minimized by shielding the individual iTMCs from each other. This can be achieved by the introduction of bulky side groups to the periphery of the complex.^[8,10] In addition, hydrophobic bulky groups in the iTMC can also increase the stability of the LECs as they render the complex less susceptible to interaction with water.^[23,24] That interaction has been identified as the primary reason for the low stability of ruthenium-based LECs.^[25–27] Three heteroleptic iridium complexes combining intracation interligand interactions with bulky groups in the periphery were prepared, [Ir(ppy)₂(Meppbpy)]PF₆ (**2**, ppy = 2-phenylpyridine; Meppbpy = 4-(3,5-dimethoxyphenyl)-6-phenyl-2,2'-bipyridine), [Ir(ppy)₂(C₁₀ppbpy)]PF₆ (**3**, C₁₀ppbpy = 4-(3,5-bis(decyloxy)phenyl)-6-phenyl-2,2'-bipyridine), and [Ir(ppy)₂(G1ppbpy)]PF₆ (**4**, G1ppbpy = 4-(3,5-bis(3,5-bis(dodecyloxy)benzyloxy)phenyl)-6-phenyl-2,2'-bipyridine), and are presented in Figure 1.

All complexes contain a phenyl group at the 6-position of the neutral 2,2'-bipyridine (bpy) ligand, which holds an additional, increasingly bulky substituent on its 4-position. The phenyl group allows for an intramolecular π - π stacking, which we have shown to be beneficial for the complex stability in the device. The additional substituent increases the intersite distance between the cations in the film, reducing the quenching of the excitons due to their

migration over the complexes, which is expected to lead to an increase of the efficiency of the LECs. Indeed, LEC devices employing complexes **2** and **3** show shorter turn-on times, higher efficiencies and luminances, and, surprisingly, also demonstrate longer device stabilities than devices employing the reference complex **1**. However, no electroluminescence behavior was observed from the devices using complex **4**, which shows the limitation of this strategy.

2. Results and Discussion

2.1. Synthesis

The presented complexes were prepared using methods similar to those for other [Ir(ppy)₂L]⁺ species. However, the dendronized 6-phenyl-2,2'-bipyridine ligands were prepared using a “green” solvent-free method developed for aldol condensation and Michael addition to give ligand Meppbpy.^[28–30] After demethylation of Meppbpy by heating with molten pyridinium chloride,^[31–33] the free phenolic hydroxyl groups were reacted with an appropriate electrophile to give the desired ligands C₁₀ppbpy and G1ppbpy (bearing a 1st generation Fréchet-type dendron). Details concerning the synthesis and the characterization of these complexes can be found in the experimental section.

2.2. Molecular Structure: Ground-State Characterization by DFT Calculations

The stability of iTMCs depends, at least partly, on their molecular structure and, in particular, on the ability to form π - π intramolecular interactions.^[19–21] We were unable to obtain X-ray quality crystals of complexes **2–4**. Instead, density functional theory (DFT) calculations were performed at the B3LYP/(6-31G** + LANL2DZ) level to fully optimize the structure of complexes **1–3** both in the ground and the excited electronic states (see the experimental section for details).

In the ground state (S_0), the pendant phenyl ring of the bpy ligand stacks face-to-face with the phenyl ring of the adjacent ppy ligand. The average stacking distance between the phenyl rings calculated for complexes **2** and **3** (~ 3.8 Å) is similar to the X-ray value reported for reference compound **1** (3.5 Å).^[19] Similar results are to be expected for complex **4**, which was not calculated due to the larger size of the substituent in the 4-position. Hence, calculations indicate that complexes **2–4** maintain the π - π intramolecular interaction observed for **1**. This interaction is also preserved in the excited states as we mention in the next sections.

Figure 2 displays the atomic orbital composition of the highest-occupied and the lowest-unoccupied molecular orbitals (HOMO and LUMO) of complex **2**. The same composition of the frontier molecular orbitals is computed for complexes **1** and **3** and is expected for complex **4**. As already reported for analogous cyclometallated Ir-iTMCs,^[15,17,34–37] the HOMO is composed of a mixture of Ir(III) d π orbitals (t_{2g}) and phenyl π orbitals of the ppy ligands and the LUMO resides on the diimine ligand showing no overlap with the HOMO. For the three complexes (**1–3**), the HOMO shows almost identical percentages of metal character

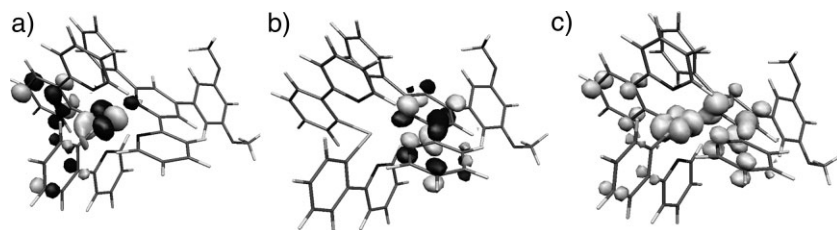


Figure 2. Electronic density contours (0.06 e bohr^{-3}) calculated for the HOMO (a) and the LUMO (b) of complex **2** in the ground state S_0 . c) Spin density distribution (0.06 e bohr^{-3}) calculated for complex **2** in the excited state 3T_1 .

(45% for **1**, 48% for **2**, and 46% for **3**) and lies at very similar energies (-7.70 , -7.65 , and -7.58 eV , respectively). The LUMO is also calculated at similar energies (-4.86 , -4.74 , and -4.63 eV for **1**, **2**, and **3**, respectively). Therefore, theoretical calculations predict similar HOMO–LUMO energy gaps for the three complexes (**1**: 2.84 eV , **2**: 2.91 eV , **3**: 2.95 eV) and similar emission wavelengths.

2.3. Electrochemical Properties

Figure 3 depicts the electrochemical characteristics of complexes **1–4** as determined by cyclic voltammetry (CV) and the measured redox potentials are listed in Table 1. The four complexes each exhibit a reversible ligand-based reduction peak at ca. -1.75 V and a nearly reversible metal-centered oxidation peak at ca. $+0.80 \text{ V}$

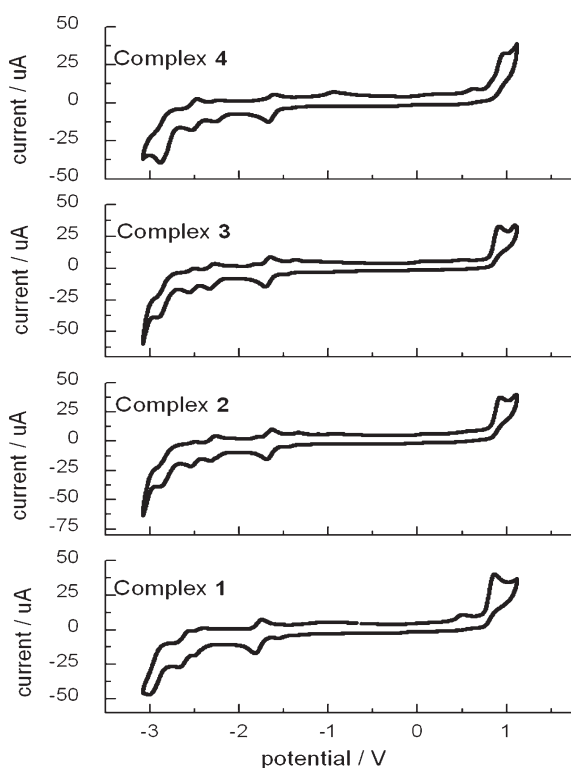


Figure 3. CV data for complexes **1–4** in de-aerated DMF solution containing $0.1 \text{ M } [{}^t\text{Bu}_4\text{N}][\text{PF}_6]$ as supporting electrolyte, internal reference Fc/Fc^+ .

versus Fc/Fc^+ (Fig. 3). Additional ligand-centered reductions are observed at more negative potentials with varying degrees of reversibility. Despite the size of the added bulky groups, no aggregation effect is observed for complexes **2–4** in dimethylformamide (DMF) solution at room temperature although some anomalies were observed in CH_2Cl_2 . First scan data of compounds **3** and **4** were also anomalous, consistent with the previously reported strong interactions of compounds of this type with graphite surfaces.^[38,39]

The electrochemical gaps ($\Delta E_{1/2}^{\text{redox}} = E_{1/2}^{\text{ox}} - E_{1/2}^{\text{red}}$) found for complexes **1** (2.60 V), **2** (2.54 V), and **3** (2.55 V) are similar to the HOMO–LUMO energy gaps obtained from DFT calculations (2.84 , 2.91 , and 2.95 eV , respectively). Therefore, it can be presumed that the oxidation process is metal-centered while the reduction occurs on the bpy ligand. As expected, the added bulky groups do not significantly affect the electrochemical properties, and the maximum PL emission is thus expected at similar wavelength values.

2.4. Photophysical Properties and Excited Triplet States

The four complexes are all yellow and exhibit a broad absorption centered at $\sim 380 \text{ nm}$ ($\epsilon = 5\,000\text{--}10\,000 \text{ L mol}^{-1} \text{ cm}^{-1}$). The PL emission spectra recorded in de-aerated acetonitrile solution show unstructured broad bands with similar emission maxima around 595 nm (Fig. 4, Table 1). The unstructured shape of the emission bands is typical for metal-to-ligand charge transfer (MLCT) electronic excitations, however, it is well known that these iridium complexes also exhibit ligand-to-ligand charge transfer (LLCT) electronic contributions.^[15,34–37]

To investigate the nature of the emitting excited state, DFT calculations at the unrestricted UB3LYP level were used for fully optimizing the electronic and molecular structures of the lowest triplet state (3T_1) of complexes **1–3**. Similar results are expected for complex **4**. The 3T_1 state mainly results from the HOMO \rightarrow LUMO monoexcitation and is computed to lie 2.23 (**1**), 2.28 (**2**), and 2.29 eV (**3**) above S_0 (adiabatic energy differences, Fig. 5c, E_2). Excitation to the 3T_1 state implies an electron transfer from the Ir-ppy environment to the substituted bpy ligand. This is illustrated in Figure 2c by the unpaired-electron spin density distribution calculated for complex **2**, which perfectly matches the topology of the HOMO \rightarrow LUMO excitation (Fig. 2a and b) in which the 3T_1 state originates. The electron transfer associated with the excitation to the 3T_1 state causes a similar contraction of the coordination sphere for the three complexes. This contraction does not affect the intramolecular π -stacking, which is preserved for the 3T_1 state (average stacking interaction of $\sim 3.8 \text{ \AA}$). The spin densities calculated for 3T_1 are very similar (Ir: 0.52 , ppy: 0.25 and 0.12 , pbpy: 1.10 for **1**; Ir: 0.49 , ppy: 0.25 and 0.12 , Meppbpy: 1.13 for **2**; Ir: 0.48 , ppy: 0.26 and 0.13 , $\text{C}_{10}\text{ppbpy}$: 1.12 for **3**) and confirm the mixed ${}^3\text{MLCT}/{}^3\text{LLCT}$ character of the lowest triplet state. The CT nature of the emitting state is in agreement with the broad and unstructured aspect of the emission band observed at $\lambda_{\text{max}} \sim 595 \text{ nm}$ (2.08 eV) for the three complexes (Fig. 4, top). To estimate the phosphorescence emission energy, the vertical energy

Table 1. Photophysical and electrochemical properties of complexes 1–4.

Complex	Emission (298 K) [a]					V_{oxd} [V] [f]	V_{red} [V] [f]
	λ_{max} [nm]	PLQE _{sol} [b]	PLQE _{dev} [c]	PLQE _{film} [d]	τ [μs] [e]		
1	595	0.03	0.21	0.37	0.50	0.81	−1.79, −2.47, −2.62
2	593	0.05	0.24	0.44	0.19	0.80	−1.74, −2.37, −2.60, −2.92
3	595	0.07	0.34	0.47	0.15	0.80	−1.75, −2.37, −2.59, −2.90
4	595	0.10	0.38	0.51	0.13	0.83	−1.74, −2.60, −2.92

[a] $\lambda_{\text{exc}} = 355$ nm. [b] De-aerated CH_3CN solution (10^{-4} M). [c] Iridium complex plus 1-butyl-3-methylimidazolium hexafluorophosphate in 4:1 molar ratio. [d] 5 wt % in PMMA. [e] Emission lifetime in de-aerated CH_3CN solution $\pm 10\%$. [f] In DMF solution versus Fc/Fc^+ .

difference between $^3\text{T}_1$ and S_0 was computed by performing a single-point calculation of S_0 at the optimized minimum-energy geometry of $^3\text{T}_1$. Calculations lead to vertical emission energies of 2.02 eV for 1, 1.88 eV for 2, and 1.97 eV for 3, in reasonably good agreement with the experimental values for the maximum emission.

The main photophysical difference between the four complexes is the increase in the PLQE and the decrease of the excited-state

lifetimes on going from 1 to 4 (Table 1). The increase of the PLQE is observed both in solution and in diluted or concentrated thin films. In concentrated films of the same composition as used in the LEC devices, the PLQE value increases with the size of the bulky substituents (from 0.21 for 1 to 0.38 for 4). Therefore, the presence of large substituents in the periphery of the complexes results in the desired increase in PLQE, most likely due to a decreased quenching of excitons. Furthermore, the excited-state lifetimes upon excitation at 355 nm decrease approximately by a factor of 4 from complex 1 to 4 (Table 1). Therefore, the radiative rate constant (k_r) increases with the use of bulky groups. These data indicate that the bulky substituents enhance the photophysical properties of the iridium complexes without modifying the nature of the emitting triplet state and its maximum emission wavelength. Hence, higher efficiencies are expected in LECs using this new family of bulky complexes (2–4) when compared to LECs using reference complex 1.

One of the deactivation pathways of the phosphorescent emission from $^3\text{T}_1$ in iTMCs is the population of the metal-centered (^3MC) triplet excited states.^[40–42] Metal-centered states

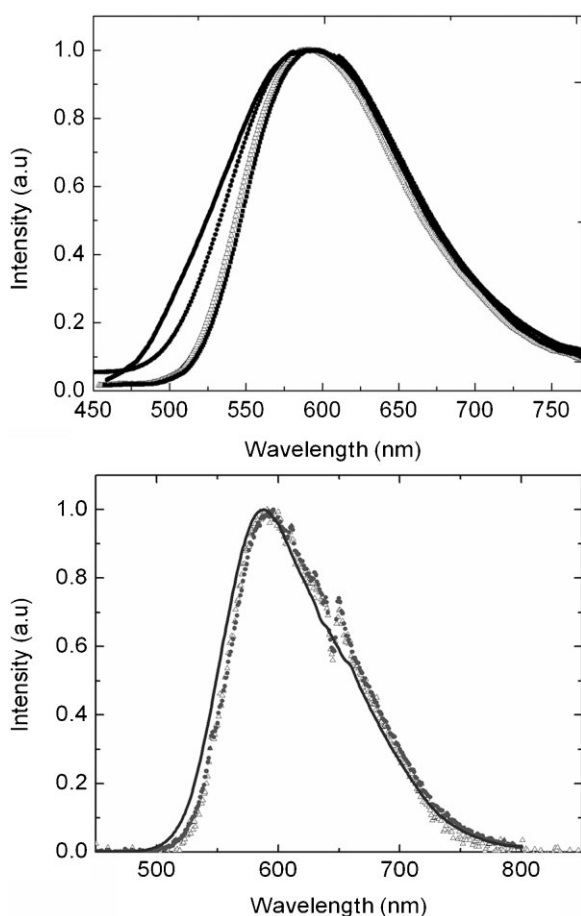


Figure 4. Top: emission spectra of 1 (solid line), 2 (full circles), 3 (open triangles), and 4 (full squares) in de-aerated CH_3CN solution. Bottom: electroluminescence spectra of LECs ITO/PEDOT:PSS/[Ir-complex][PF₆]:IL(4:1)/Al employing iTMC 1 (solid line), 2 (full circles), and 3 (open triangles) at an applied bias of 3 V.

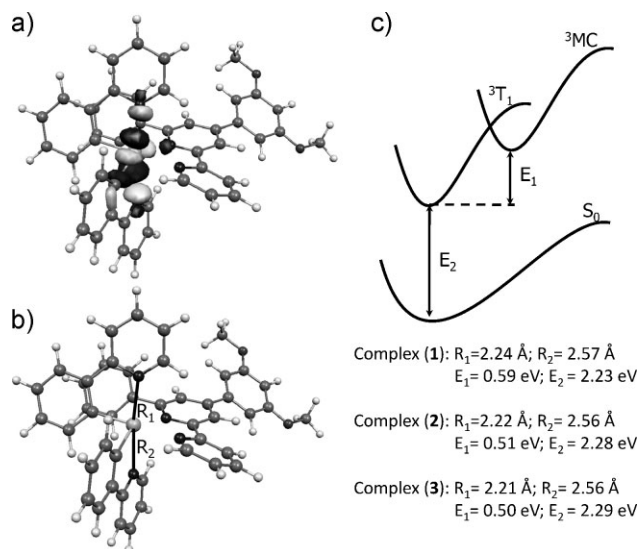


Figure 5. a) Electron density contours (0.06 e bohr⁻³) calculated for the unoccupied e_g molecular orbital of complex 2 showing σ -antibonding interactions along the vertical $\text{N}_{\text{ppy}}\text{--Ir--N}_{\text{ppy}}$ axis. b) Minimum-energy structure calculated for the ^3MC state of complex 2, where R_1 and R_2 are the lengths of the $\text{Ir--N}_{\text{ppy}}$ bonds. c) Schematic energy diagram showing the adiabatic energy differences calculated between the S_0 , $^3\text{T}_1$, and ^3MC states. The values computed for R_1 and R_2 are given for the ^3MC state.

result from the excitation of an electron from the occupied t_{2g} ($d\pi$) HOMO to the unoccupied e_g ($d\sigma^*$) orbitals of the metal^[41] and are assumed to be the origin of the degradation process for the complex $[\text{Ru}(\text{bpy})_3]^{2+}$ in solution as well as in LECs.^[25,26,40–42] In complex 1, the ^3MC states are calculated after geometry relaxation to lie approximately 0.6 eV above the lowest energy $^3\text{T}_1$ state. Although these states are somewhat higher in energy than those on $[\text{Ru}(\text{bpy})_3]^{2+}$, they are still accessible. Hence, we assume that for iridium(III)-based iTMCs, the relative position of the ^3MC states is related to the complex stability in the device. For complexes 2 and 3, ^3MC states are computed to lie 0.5 eV above the emitting triplet state ($^3\text{T}_1$), similar to what is obtained for complex 1 (Fig. 5c, E_1). Therefore, the probability of populating the ^3MC states should be approximately the same for the three complexes.

The geometries of the ^3MC states were fully relaxed starting from the optimized geometry of S_0 with Ir–N_{ppy} bond distances lengthened to 2.70 Å since, as sketched in Figure 5a, the relevant e_g ($d\sigma^*$) orbital is σ -antibonding between the metal and the nitrogens of the ppy ligands. Electron promotion to this orbital, however, causes a very different effect on the Ir–N_{ppy} bonds. While the Ir–N_{ppy} bond of the ppy ligand not involved in the intramolecular π -stacking (R_2 in Fig. 5b) drastically changes from 2.08 Å in S_0 to \sim 2.55 Å, the π -stacking (\sim 3.9 Å) prevents the weakening of the Ir–N_{ppy} bond involved in this interaction (R_1 in Fig. 5b) and this bond only lengthens to \sim 2.20 Å. The pendant phenyl ring in the 6-position thus exerts a cage effect that restricts the opening of the structure of the complex in the excited ^3MC state and only one of the N_{ppy} atoms is virtually de-coordinated. This supramolecular cage effect makes complexes 1–4 more robust reducing the possibility of ligand-exchange degradation reactions.

2.5. Electroluminescent Devices

LECs were prepared from complexes 2, 3, and 4 using the methodology previously reported.^[19] An indium tin oxide (ITO)-covered substrate was coated with a 0.1- μm spin-coated layer of poly(3,4-ethylenedioxythiophene):poly(styrene sulfonic acid) (PEDOT:PSS) followed by a 90-nm spin-coated layer of a 4:1 molar mixture of the iTMC and the ionic liquid 1-butyl-3-methylimidazolium hexafluorophosphate and finally an aluminum layer was evaporated as cathode. The ionic liquid is incorporated to improve the turn-on time, the time to reach the maximum luminance (t_{on}) of the device.^[43] Details concerning the device preparation and characterization can be found in the experimental section.

The devices employing complex 4 showed neither an increase in current density nor luminance at applied biases of 3 and 4 V over a period of 48 h. The reason for the inactivity of these devices is not clear, but might be due to the very large intercomplex distance resulting from the bulky substituent.^[10,44] As LECs are unstable

when operated at higher biases, the devices using complex 4 were not further investigated. The devices using complexes 2 and 3 showed bright orange electroluminescence when biased at 3 V (Fig. 4, bottom). They exhibited the typical responses of LECs, namely a slow rise of the current density and luminance upon applying a low bias to the device. The turn-on times are very long (77 and 33 h for devices using complexes 2 and 3, respectively) but considerably lower than that observed from the reference device employing complex 1 (237 h) (Fig. 6, Table 2). The extremely long t_{on} for the device using complex 1 was reported earlier but is still not fully understood.^[19] One suggestion is that the complex crystallizes in nanometer-sized domains in the thin film, which would severely hinder the movement of the counterions as they are ordered in laminas. It is not easy to verify the morphology of thin films of these complexes. It has only been rigorously analyzed in the case of $[\text{Ru}(\text{bpy})_3]^{2+}$ using synchrotron X-ray radiation. In that study it was established that a spin-coated film did indeed consist of nanoscale crystalline domains.^[45] Assuming that in these complexes some crystallization takes place, the long t_{on} values can be rationalized. The lower t_{on} values measured for devices using complexes 2 and 3 hint towards a thin film packing of the complex cations that yields more “free” anions. Irrespective of the exact origin of the slow responses, it is possible to improve them by applying short pulses of higher voltages, and to reach values interesting for practical applications.^[19,44,46] To allow for an exact comparison between the devices using the different complexes, this pre-biasing was not applied in this work.

The efficiencies found for the devices using complexes 2 and 3 were significantly higher than those obtained from the devices using complex 1 (Table 2). This is expected in view of the difference in PLQE for films of the complexes using the device composition (Table 1). In view of Equation (1), the EQE of the LECs are mainly determined by the PLQE values. According to this simple relationship, the EQEs for the devices using complexes 1, 2, and 3 should then be 4.6%, 5.3%, and 7.5%, respectively. These predicted values are higher than those obtained experimentally for the different LECs, indicating that either the outcoupling factor is not accurate or that not all charge carriers recombine. In particular, the LECs using 1 have a significantly lower experimental EQE, whereas for those using 3 the error between the predicted and observed EQE is not that large, indicating that the latter represents a rather optimized device configuration.

The highest current densities are observed for the devices making use of complex 1 and are approximately four times higher than those measured for devices using complex 2 or 3 (Fig. 6). However, due to the increased device efficiencies, the maximum luminances obtained for the devices using 2 and 3 are significantly higher than that found for the reference device, reaching 183 and 284 cd m^{-2} , respectively, at only 3 V bias.

The stability, when expressed as the time to reach half of the maximum brightness (lifetime or $t_{1/2}$), decreases with faster t_{on} .

Table 2. Performance of LEC devices at a driving voltage of 3 V.

Complex	t_{on} [h]	Luminance _{max} [cd m^{-2}]	$t_{1/2}$ [h]	E_{tot} [J]	Efficacy [cd A^{-1}]	Power efficiency [lm W^{-1}]	EQE [%]
1	237	109	1290	13.6	3.1	3.3	1.3
2	77	183	950	17.2	8.2	8.6	3.4
3	33	284	660	17.4	14.7	15.3	6.1

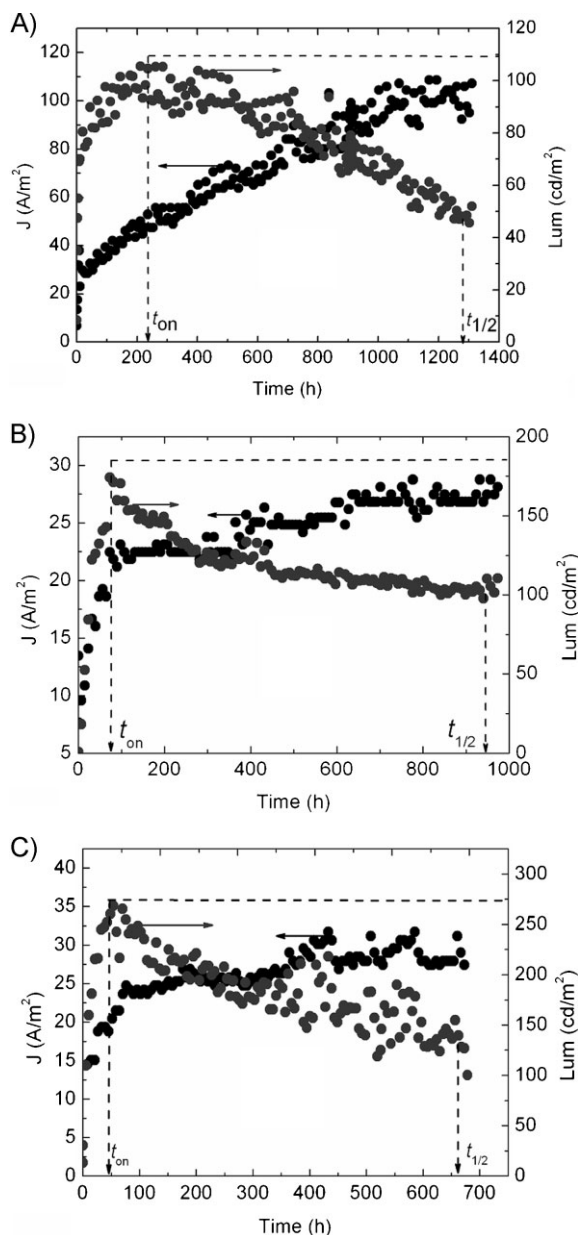


Figure 6. Current density and luminance data for three ITO/PEDOT:PSS/iTMC:IL(4:1)/Al LECs at an applied bias of 3 V employing: A) [Ir(ppy)₂(pb-ppy)][PF₆] (1), B) [Ir(ppy)₂(Meppbpy)][PF₆] (2), and C) [Ir(ppy)₂(C₁₀ppbpy)][PF₆] (3).

This trend, although not understood, has been observed for many LECs.^[1,17,43] However, as mentioned in the work by Kalyuzhny et al., $t_{1/2}$ is not a good value to compare the stability of LECs and can only be used when the maximum luminances of the different devices are similar.^[25] It is known that in electroluminescent devices, the time to reach half of the initial luminance depends strongly on the initial luminance chosen. Since the devices described in this work have very different maximum luminances at the same driving voltages, the device stability cannot be compared using the $t_{1/2}$ values. In their work, Kalyuzhny et al. proposed an

alternative method, where the stability is expressed as the total emitted energy (E_{tot}) up to the time the luminance reaches one-fifth of the maximum value ($t_{1/5}$) for a cell area of 3 mm².^[25] When the devices are compared in this way, we obtain the surprising result that the devices using 2 or 3 show higher values of the total emitted energy (17.2 and 17.4 J, respectively) than the reference device (13.6 J). Hence, the introduction of the bulky side groups not only increases the device efficiency but also increases the device stability.

3. Conclusion

In conclusion, three ionic iridium(III) complexes exhibiting intramolecular π - π interactions between the pendant phenyl ring of a 6-phenyl-2,2'-bipyridine ligand and one of the phenyl rings of the ppy ligands and containing bulky groups of increasing size were prepared. With increasing size of the bulky side groups, the PL quantum yield of the complexes increases both in dilute solution and in concentrated films. When used to prepare simple LECs, complexes 2 and 3 resulted in efficient devices with high luminance values. Additionally, the total emitted energy during the device operation was larger than that obtained from devices based on the reference complex 1, which does not contain bulky groups. Hence, substituting the complex on the periphery with large (electronically inactive) groups greatly improves the efficiency, the luminance, and the stability of the LECs employing them. It appears that this strategy cannot be extended indefinitely, as we observed no electroluminescence from the device employing complex 4 with the largest side group.

4. Experimental

General: All chemicals were commercially available and of reagent grade and were used without further purification. The solvents (puriss grade) were purchased from Fluka. 2-Phenylpyridine and hydrated iridium trichloride were used as received from Aldrich and Johnson Matthey, respectively. Preparative column chromatography was done using Fluka silica gel 60 (0.040–0.063 mm) or Merck aluminum oxide 90 standardized unless otherwise stated. Freshly distilled solvents were used. Steady-state fluorescence spectra were measured on a Photon Technology spectrofluorometer equipped with a lamp power supply (LPS-220B) working at room temperature. The excited-state lifetimes were measured from fresh solutions, which were degassed by Ar bubbling for 30 min. They were deduced from time-resolved absorption spectroscopy utilizing a laser flash-photolysis system based on a pulsed Nd:YAG laser using 355 nm as exciting wavelength. The single pulses were approximately 10 ns duration and the energy was approximately 15 mJ per pulse. A Lo255 Oriel xenon lamp was employed as the detecting light source. The laser flash-photolysis apparatus consisted of the pulsed laser, the Xe lamp, a 77200 Oriel monochromator, and an Oriel photomultiplier (PMT) system made up of 77348 PMT power supply. The oscilloscope was a TDS-640A Tektronix. The output signal from the oscilloscope was transferred to a personal computing machine.

The thin-film quantum yield measurements were performed in a nitrogen environment and determined on a thin film (100 nm) dispersed in poly(methyl methacrylate) (PMMA) (5 wt%) and on thin films (70 nm) with the same configuration than the LEC device with an ionic liquid at 4:1 molar ratio of Ir-iTMC/1-butyl-3-methylimidazolium hexafluorophosphate for the four complexes (1, 2, 3, and 4) using the quantum yield measurement system from Hamamatsu, model C9920-01. Voltammetric measurements employed a PC-controlled Eco Chemie Autolab PGSTAT 20 electrochemical

workstation. CVs were obtained at a scan rate of 100 mV s⁻¹ using 0.1 M TBAPF₆ as supporting electrolyte in DMF. Glassy carbon, platinum mesh, and silver wire were employed as working, counter, and pseudo reference electrodes, respectively. At the end of each measurement, the Fc⁺/Fc potential was measured and used as an internal reference. NMR spectra were measured on Bruker AM 250 MHz, Bruker DRX-400 MHz, or Bruker DRX-500 MHz spectrometers and the reported chemical shifts are relative and internally referenced to either TMS or the residual peak of the solvent.

Synthesis: a) Preparation of Meppbpy. Acetophenone (6.69 g, 55.7 mmol, 1.00 eq.), 3,5-dimethoxybenzaldehyde (9.25 g, 55.7 mmol, 1.00 eq.), and powdered NaOH (2.23 g, 55.7 mmol, 1.00 eq.) were combined using a mortar and a pestle. The yellow mixture was ground and became stickier, although it never solidified even after 30 min of grinding. 2-Acetylpyridine (6.74 g, 55.7 mmol, 1.00 eq.) was added and everything was mixed together until the material was too viscous to grind. The mortar with the substance was placed in a desiccator overnight. The following day, the ochre mixture was powdered and transferred to a round-bottom flask. Ammonium acetate (28.9 g, 0.375 mol, 6.70 eq.) and PEG-300 (90 mL) were added and the mixture heated to 100 °C and stirred for 16 h. The brown solution was then cooled down to room temperature and water (300 mL) was added whereupon a sticky ochre material precipitated. The supernatant solution was decanted, the residue was washed twice with water (100 mL each) and dissolved in Et₂O (200 mL). The brown solution was evaporated to dryness to give a mixture of a solid and an oil. Everything was dissolved in CH₂Cl₂ and washed once with NaHCO₃ (half saturated) and twice with water. The organic layer was dried (MgSO₄) and evaporated to dryness to give a brown, sticky oil. The crude material was purified by column chromatography (silica gel 60; CH₂Cl₂ → Et₂O:hexane = 1:1 → 2:1) followed by a subsequent column chromatography (silica gel 60; Et₂O:hexane = 1:2 → 2:3 → 1:1 → 2:1) and recrystallized from n-heptane affording the desired product as an off-white solid (4.97 g, 13.5 mmol, 24%). R_f (TLC, silica gel, Et₂O:hexane = 2:1): 0.5; ¹H NMR (500 MHz, CDCl₃, δ): 8.72 (d, ³J = 4.6 Hz, 1H, H^{6(A)}), 8.69 (d, ³J = 7.9 Hz, 1H, H^{3(A)}), 8.62 (d, ⁴J = 2.1 Hz, 1H, H^{3(B)}), 8.20 (d, ³J = 7.2 Hz, 2H, H^{2(C)}), 7.95 (d, ⁴J = 1.3 Hz, 1H, H^{5(B)}), 7.88 (t, ³J = 7.7 Hz, 1H, H^{4(A)}), 7.53 (t, ³J = 7.5 Hz, 2H, H^{3(C)}), 7.46 (t, ³J = 7.3 Hz, 1H, H^{4(C)}), 7.36 (t, ³J = 6.1 Hz, 1H, H^{5(A)}), 6.94 (d, ⁴J = 2.2 Hz, 2H, H^{2(D)}), 6.57 (t, ⁴J = 2.1 Hz, 1H, H^{4(D)}), 3.89 (s, 6H, OCH₃); ¹³C NMR (126 MHz, CDCl₃, δ): 161.43 (C^{3(D)}), 157.30 (C^{6(B)}), 156.47 (C^{2(A)}/C^{2(B)}), 156.40 (C^{2(A)}/C^{2(B)}), 150.56 (C^{4(B)}), 149.07 (C^{6(A)}), 141.18 (C^{1(D)}), 139.56 (C^{1(C)}), 137.06 (C^{4(A)}), 129.28 (C^{4(C)}), 128.91 (C^{3(C)}), 127.24 (C^{2(C)}), 124.02 (C^{5(A)}), 121.81 (C^{3(A)}), 118.89 (C^{5(B)}), 117.83 (C^{3(B)}), 105.65 (C^{2(D)}), 101.05 (C^{4(D)}), 55.76 (OCH₃); IR (solid): ν = 3055 (w), 3009 (w), 2976 (w), 1954 (w), 1595 (s), 1583 (s), 1545 (s), 1445 (s), 1389 (s), 1331 (m), 1286 (m), 1200 (s), 1151 (s), 1063 (s), 987 (w), 928 (w), 906 (w), 849 (m), 825 (s), 791 (s), 770 (s), 731 (m), 689 (s), 662 (s), 652 (s), 640 (s), 617 (s), 579 (m) cm⁻¹; MS (ESI, m/z): 759.9 [2M+Na]⁺ (calc. 759.3); Anal. calcd. for C₂₄H₂₀N₂O₂ (368.43): C 78.24, H 5.47, N 7.60; found: C 78.03, H 5.47, N 7.45.

b) Preparation of 4-(3,5-dihydroxyphenyl)-6-phenyl-2,2'-bipyridine. Meppbpy (4.27 g, 11.6 mmol, 1.00 eq.) and pyridine hydrochloride (67 g, 0.58 mol, 50 eq.; as prepared by slow addition of equimolar amounts of aqueous HCl to ice-cooled pyridine followed by water removal under vacuo) were mixed and stirred at reflux for 2.5 h under an inert atmosphere of N₂. The reaction mixture was cooled down from ca. 250 to ca. 160 °C (still molten) and poured into water (2 L) whereupon a white solid immediately precipitated. Measuring with a pH-probe, the aqueous phase was neutralized with saturated aqueous NaHCO₃ (ca. 550 mL) from pH 2.7 to 6.2. The precipitate was filtered off, washed well with water (1 L), powdered and dried in the desiccator yielding the desired product as an off-white powder (4.18 g, M-H₂O, 11.5 mmol, 99%). R_f (TLC, silica gel, CH₂Cl₂:MeOH = 10:1): 0.5; ¹H NMR (500 MHz, CD₃OD, δ): 8.67 (d, ³J = 4.1 Hz, 1H, H^{6(A)}), 8.60 (d, ³J = 8.0 Hz, 1H, H^{3(A)}), 8.43 (d, ⁴J = 1.2 Hz, 1H, H^{3(B)}), 8.20 (d, ³J = 7.3 Hz, 2H, H^{2(C)}), 8.01 (d, ⁴J = 1.3 Hz, 1H, H^{5(B)}), 7.98 (td, ³J = 7.8 Hz, ⁴J = 1.6 Hz, 1H, H^{4(A)}), 7.52 (t, ³J = 7.5 Hz, 2H, H^{3(C)}), 7.48–7.43 (m, 2H, H^{5(A)} + H^{4(C)}), 6.78 (d, ⁴J = 2.1 Hz, 2H, H^{2(D)}), 6.40 (t, ⁴J = 2.0 Hz, 1H, H^{4(D)}); ¹³C NMR (126 MHz, CD₃OD, δ): 160.62 (C^{3(D)}), 158.91 (C^{6(B)}), 157.75 (C^{2(A)}), 157.29 (C^{2(B)}), 152.25 (C^{4(B)}), 150.17 (C^{6(A)}), 141.85 (C^{1(D)}), 140.70 (C^{1(C)}), 138.96 (C^{4(A)}), 130.41 (C^{4(C)}),

129.96 (C^{3(C)}), 128.30 (C^{2(C)}), 125.52 (C^{5(A)}), 123.24 (C^{3(A)}), 119.49 (C^{5(B)}), 118.55 (C^{3(B)}), 106.73 (C^{2(D)}), 104.60 (C^{4(D)}); IR (solid): ν = 3306 (w), 3198 (w), 3061 (w), 2644 (w), 1981 (w), 1794 (w), 1686 (w), 1587 (s), 1549 (s), 1497 (m), 1475 (m), 1443 (m), 1373 (w), 1344 (w), 1304 (m), 1259 (w), 1159 (s), 1088 (w), 1001 (s), 829 (s), 787 (m), 770 (s), 727 (m), 687 (s), 660 (s), 636 (s), 617 (s) cm⁻¹; MS (ESI, m/z): 703.6 [2M+Na]⁺ (calc. 703.2); 363.5 [M+Na]⁺ (calc. 363.1); Anal. calcd. for C₂₂H₁₆N₂O₂·H₂O (358.39): C 73.73, H 5.06, N 7.82; found: C 74.15, H 5.05, N 7.77.

c) Preparation of 4-(3,5-bis(decyloxy)phenyl)-6-phenyl-2,2'-bipyridine. A mixture of 1-bromodecane (0.38 mL, 1.8 mmol, 2.5 eq.), 4-(3,5-dihydroxyphenyl)-6-phenyl-2,2'-bipyridine (250 mg, 0.734 mmol, 1.00 eq.), 18-crown-6 (39 mg, 0.15 mmol, 0.20 eq.), and K₂CO₃ (406 mg, 2.94 mmol, 4.00 eq.) in dry acetone (3 mL) was placed in a microwave reactor and heated for 60 min at 120 °C under a pressure of 7 bar. The solvent was evaporated to dryness and water (50 mL) was added to the residue. This was extracted three times with ethyl acetate (each 50 mL). The combined organic layers were dried (MgSO₄) and evaporated to dryness. The crude material was purified by column chromatography (Alox 90; hexane:ethyl acetate:CH₂Cl₂ = 30:1:2), followed by a subsequent column chromatography (silica gel 60; hexane:ethyl acetate = 8:1) yielding the desired product as a white solid (428 mg, 0.689 mmol, 94%). R_f (TLC, silica gel, hexane:ethyl acetate = 8:1): 0.4; ¹H NMR (500 MHz, CDCl₃, δ): 8.72 (d, ³J = 4.7 Hz, 1H, H^{6(A)}), 8.69 (d, ³J = 7.9 Hz, 1H, H^{3(A)}), 8.61 (s, 1H, H^{3(B)}), 8.21 (d, ³J = 7.5 Hz, 2H, H^{2(C)}), 7.96 (s, 1H, H^{5(B)}), 7.87 (t, ³J = 7.7 Hz, 1H, H^{4(A)}), 7.53 (t, ³J = 7.6 Hz, 2H, H^{3(C)}), 7.46 (t, ³J = 7.3 Hz, 1H, H^{4(C)}), 7.34 (dd, ³J = 7.3 Hz, ³J = 4.9 Hz, 1H, H^{5(A)}), 6.93 (d, ⁴J = 1.8 Hz, 2H, H^{2(D)}), 6.56 (t, ⁴J = 1.9 Hz, 1H, H^{4(D)}), 4.03 (t, ³J = 6.5 Hz, 4H, OCH₂CH₂CH₂), 1.86–1.78 (m, 4H, OCH₂CH₂CH₂), 1.53–1.45 (m, 4H, OCH₂CH₂CH₂), 1.42–1.21 (m, 24H, OCH₂CH₂CH₂(CH₂)₆CH₃), 0.88 (t, ³J = 6.8 Hz, 6H, O(CH₂)₉CH₃); ¹³C NMR (126 MHz, CDCl₃, δ): 160.95 (C^{3(D)}), 157.20 (C^{6(B)}), 156.54 (C^{2(A)}/C^{2(B)}), 156.37 (C^{2(A)}/C^{2(B)}), 150.62 (C^{4(B)}), 149.19 (C^{6(A)}), 140.98 (C^{1(D)}), 139.63 (C^{1(C)}), 137.01 (C^{4(A)}), 129.21 (C^{4(C)}), 128.88 (C^{3(C)}), 127.24 (C^{2(C)}), 123.93 (C^{5(A)}), 121.70 (C^{3(A)}), 118.82 (C^{5(B)}), 117.73 (C^{3(B)}), 106.12 (C^{2(D)}), 101.76 (C^{4(D)}), 68.43 (OCH₂), 32.05 (O(CH₂)₉), 29.75 (O(CH₂)₉), 29.72 (O(CH₂)₉), 29.57 (O(CH₂)₉), 29.48 (O(CH₂)₉), 29.47 (O(CH₂)₉), 26.23 (OCH₂CH₂CH₂), 22.83 (O(CH₂)₉), 14.27 (O(CH₂)₉CH₃); IR (solid): ν = 3059 (w), 2922 (s), 2853 (m), 1582 (s), 1551 (m), 1466 (w), 1456 (w), 1385 (m), 1306 (m), 1259 (w), 1173 (s), 1082 (w), 1047 (m), 986 (w), 908 (w), 881 (w), 851 (w), 829 (m), 814 (w), 793 (m), 775 (m), 735 (m), 723 (m), 689 (s), 667 (m), 640 (w), 617 (w), 598 (w), 581 (w) cm⁻¹; MS (ESI, m/z): 1264.9 [2M+Na]⁺ (calc. 1263.9). Anal. calcd. for C₄₂H₅₆N₂O₂ (620.91): C 81.24, H 9.09, N 4.51; found: C 81.32, H 9.10, N 4.30.

d) Preparation of G1ppbpy. NEt₃ (22 mL, 0.16 mol, 5.0 eq.) was added to a solution of 3,5-bis(dodecyloxy)phenylmethanol (15.0 g, 31.4 mmol, 1.00 eq.) in CH₂Cl₂ (100 mL), previously cooled to -10 °C. Methanesulfonyl chloride (9.7 mL, 0.13 mol, 4.0 eq.) was added slowly over a period of 20 min, and then the reaction mixture was stirred at -10 °C for 1 h. The mixture was poured into a mixture of concentrated HCl (20 mL) and crushed ice (200 g), and extracted with CH₂Cl₂. The organic layer was washed with a saturated solution of NaHCO₃, dried with Na₂SO₄, and the solvent removed. 3,5-bis(dodecyloxy)benzyl methanesulfonate was isolated as a yellow solid (18.2 g, 32.8 mmol, 104%). A mixture of 3,5-bis(dodecyloxy)benzyl methanesulfonate (611 mg, ca. 80% pure, 0.881 mmol, 3.00 eq.), 4-(3,5-dihydroxyphenyl)-6-phenyl-2,2'-bipyridine (100 mg, 0.294 mmol, 1.00 eq.), 18-crown-6 (16 mg, 0.059 mmol, 0.20 eq.), and K₂CO₃ (162 mg, 1.18 mmol, 4.00 eq.) in dry acetone (3 mL) was placed in a microwave reactor and heated for 60 min at 100 °C under a pressure of 2 bar. The solvent was evaporated to dryness and water (50 mL) was added to the residue. This was extracted three times with ethyl acetate (each 50 mL). The combined organic layers were dried (MgSO₄) and evaporated to dryness. The crude material was purified by Alox chromatography (Alox 90; hexane:ethyl acetate:CH₂Cl₂ = 45:1:2 → 30:1:2), followed by a subsequent column chromatography (silica gel 60; hexane:ethyl acetate = 10:1) and another column chromatography (silica gel 60; hexane:ethyl acetate = 15:1) yielding the desired product as a white solid (229 mg, 0.182 mmol, 62%). R_f (TLC, silica gel, hexane:ethyl acetate = 8:1): 0.2; ¹H NMR

(500 MHz, CDCl₃, δ): 8.72 (d, ³J = 4.5 Hz, 1H, H^{6(A)}), 8.69 (d, ³J = 7.9 Hz, 1H, H^{3(A)}), 8.62 (d, ⁴J = 1.2 Hz, 1H, H^{3(B)}), 8.20 (d, ³J = 7.4 Hz, 2H, H^{2(C)}), 7.93 (d, ⁴J = 1.2 Hz, 1H, H^{5(B)}), 7.87 (td, ³J = 7.7 Hz, ⁴J = 1.7 Hz, 1H, H^{4(A)}), 7.54 (t, ³J = 7.6 Hz, 2H, H^{2(C)}), 7.46 (t, ³J = 7.3 Hz, 1H, H^{4(C)}), 7.35 (dd, ³J = 7.0 Hz, ³J = 5.2 Hz, 1H, H^{5(A)}), 7.05 (d, ⁴J = 2.1 Hz, 2H, H^{2(D)}), 6.71 (t, ⁴J = 2.0 Hz, 1H, H^{4(D)}), 6.61 (d, ⁴J = 2.0 Hz, 4H, H^{2(E)}), 6.43 (t, ⁴J = 2.0 Hz, 2H, H^{4(E)}), 5.05 (s, 4H, Ar_DOCH₂Ar_E), 3.95 (t, ³J = 6.6 Hz, 8H, OCH₂CH₂CH₂), 1.80–1.73 (m, 8H, OCH₂CH₂CH₂), 1.48–1.40 (m, 8H, OCH₂CH₂CH₂), 1.37–1.21 (m, 64H, OCH₂CH₂CH₂(CH₂)₈CH₃), 0.88 (t, ³J = 6.9 Hz, 12H, O(CH₂)₁₁CH₃); ¹³C NMR (126 MHz, CDCl₃, δ): 160.72 (C^{3(E)}), 160.56 (C^{3(D)}), 157.24 (C^{6(B)}), 156.49 (C^{2(A)}/C^{2(B)}), 156.42 (C^{2(A)}/C^{2(B)}), 150.30 (C^{4(B)}), 149.20 (C^{6(A)}), 141.06 (C^{1(D)}), 139.54 (C^{1(C)}), 138.94 (C^{1(E)}), 137.02 (C^{4(A)}), 129.24 (C^{4(C)}), 128.90 (C^{3(C)}), 127.22 (C^{2(C)}), 123.96 (C^{5(A)}), 121.69 (C^{3(A)}), 118.72 (C^{5(B)}), 117.64 (C^{3(B)}), 106.86 (C^{2(D)}), 105.90 (C^{2(E)}), 102.51 (C^{4(D)}), 101.10 (C^{4(E)}), 70.54 (Ar_DOCH₂Ar_E), 68.25 (OCH₂(CH₂)₁₀CH₃), 32.07 (OCH₂(CH₂)₁₀CH₃), 29.82 (OCH₂(CH₂)₁₀CH₃), 29.79 (OCH₂(CH₂)₁₀CH₃), 29.76 (OCH₂(CH₂)₁₀CH₃), 29.74 (OCH₂(CH₂)₁₀CH₃), 29.57 (OCH₂(CH₂)₁₀CH₃), 29.50 (OCH₂(CH₂)₁₀CH₃), 29.42 (OCH₂(CH₂)₁₀CH₃), 26.21 (OCH₂CH₂CH₂), 22.84 (OCH₂(CH₂)₁₀CH₃), 14.28 (O(CH₂)₁₁CH₃); IR (solid): ν = 3059 (w), 2918 (s), 2849 (s), 1593 (s), 1553 (w), 1450 (m), 1377 (m), 1346 (w), 1325 (w), 1296 (m), 1155 (s), 1053 (s), 1014 (w), 825 (m), 793 (w), 775 (w), 737 (w), 719 (w), 689 (w), 609 (w), 582 (w) cm⁻¹; MS (ESI, m/z): 1281.0 [M+Na]⁺ (calc. 1279.9); Anal. calcd. for C₈₄H₁₂₄N₂O₆ (1257.89): C 80.21, H 9.94, N 2.23; found: C 80.03, H 9.80, N 2.06.

e) Preparation of 2. A yellow suspension of tetrakis(2-phenylpyridine-C,N)di(μ-chloro)diiridium(III) (300 mg, 0.280 mmol, 1.00 eq.) and Meppppy (208 mg, 0.565 mmol, 2.00 eq.) in MeOH (30 mL) and CH₂Cl₂ (30 mL) was refluxed under an inert atmosphere of N₂ in the dark for 12 h. The orange solution was then cooled down to room temperature, and solid ammonium hexafluorophosphate (456 mg, 2.80 mmol, 10.0 eq.) was added to the solution. The mixture was stirred for 45 min at room temperature and then evaporated to dryness. The crude material was purified by column chromatography (Alox 90, CH₂Cl₂ → CH₂Cl₂:MeOH = 100:1) yielding the desired product as an orange solid (519 mg, 0.512 mmol, 91%). ¹H NMR (500 MHz, CD₂Cl₂, δ): 8.65 (d, J = 1.3 Hz, 1H), 8.63 (d, J = 8.2 Hz, 1H), 8.15 (t, J = 7.9 Hz, 1H), 7.92–7.81 (m, 4H), 7.77 (t, J = 7.8 Hz, 1H), 7.70 (d, J = 5.7 Hz, 1H), 7.66 (s, 1H), 7.63 (d, J = 5.7 Hz, 1H), 7.54 (d, J = 7.7 Hz, 1H), 7.40 (t, J = 6.5 Hz, 1H), 7.25 (d, J = 7.8 Hz, 1H), 7.12–7.02 (m, 2H), 6.99–6.94 (m, 4H), 6.83 (t, J = 7.5 Hz, 1H), 6.77 (t, J = 7.5 Hz, 2H), 6.68–6.50 (m, 4H), 6.40 (t, J = 7.4 Hz, 1H), 5.97 (d, J = 7.6 Hz, 1H), 5.59 (d, J = 7.6 Hz, 1H), 3.88 (s, 6H); ¹³C NMR (126 MHz, CD₂Cl₂, δ): 169.21, 167.58, 166.30, 162.23, 157.59, 157.18, 151.58, 151.34, 150.75, 149.36, 149.22, 147.26, 143.36, 143.13, 139.70, 138.56, 138.41, 138.12, 137.68, 131.81, 131.15, 130.64, 129.99, 129.46, 128.26, 128.17, 127.83, 127.82, 125.54, 124.99, 124.85, 123.78, 123.16, 122.79, 121.46, 121.15, 120.26, 120.23, 105.87, 102.89, 56.16; IR (solid): ν = 3043 (w), 2947 (w), 2843 (w), 1595 (s), 1539 (w), 1477 (m), 1394 (m), 1308 (w), 1269 (w), 1204 (m), 1155 (s), 1061 (m), 1030 (w), 935 (w), 829 (s), 789 (s), 754 (s), 725 (s), 694 (m), 667 (w), 615 (w), 579 (w), 555 (s) cm⁻¹; MS (ESI, m/z): 869.2 [M-PF₆]⁺ (calc. 869.2). Anal. calcd. for C₄₆H₃₆F₆IrN₄O₂P·0.5H₂O (1013.98): C 54.49, H 3.58, N 5.53; found: C 54.52, H 3.71, N 5.45.

f) Preparation of 3. A yellow suspension of tetrakis(2-phenylpyridine-C,N)di(μ-chloro)diiridium(III) (200 mg, 0.187 mmol, 1.00 eq.) and C₁₀ppppy (232 mg, 0.373 mmol, 2.00 eq.) in MeOH (30 mL) and CH₂Cl₂ (30 mL) was refluxed under an inert atmosphere of N₂ in the dark for 12 h. The orange solution was then cooled down to room temperature and solid ammonium hexafluorophosphate (304 mg, 1.87 mmol, 10.0 eq.) was added to the solution. The mixture was stirred for 30 min at room temperature and then evaporated to dryness. The crude material was purified by column chromatography (Alox 90, CH₂Cl₂:hexane = 1:1 → CH₂Cl₂ → CH₂Cl₂:MeOH = 100:2), followed by a subsequent column chromatography (silica gel 60; CH₂Cl₂ → CH₂Cl₂:MeOH = 100:2) yielding the desired product as an orange solid (454 mg, 0.358 mmol, 96%). R_f (TLC, silica gel, CH₂Cl₂:MeOH = 100:1): 0.3; ¹H NMR (500 MHz, CD₂Cl₂, δ): 8.66 (d, J = 1.6 Hz, 1H), 8.63 (d, J = 8.2 Hz, 1H), 8.18 (t, J = 7.9 Hz, 1H), 7.95 (d, J = 4.8 Hz, 1H), 7.91–7.86 (m, 3H), 7.81 (td, J = 8.0 Hz, J = 1.3 Hz, 1H),

7.74 (d, J = 5.7 Hz, 1H), 7.70 (d, J = 1.7 Hz, 1H), 7.63 (d, J = 5.6 Hz, 1H), 7.58 (d, J = 7.7 Hz, 1H), 7.45 (t, J = 6.5 Hz, 1H), 7.29 (d, J = 7.8 Hz, 1H), 7.14–7.07 (m, 2H), 7.01 (t, J = 7.5 Hz, 2H), 6.97 (d, J = 2.0 Hz, 2H), 6.87 (td, J = 7.6 Hz, J = 1.1 Hz, 1H), 6.80 (t, J = 7.6 Hz, 2H), 6.70–6.53 (m, 4H), 6.44 (t, J = 7.4 Hz, 1H), 6.01 (d, J = 7.7 Hz, 1H), 5.63 (d, J = 7.5 Hz, 1H), 4.07 (t, J = 6.5 Hz, 4H), 1.87–1.80 (m, 4H), 1.54–1.47 (m, 4H), 1.44–1.26 (m, 24H), 0.92 (t, J = 6.9 Hz, 6H); ¹³C NMR (126 MHz, CD₂Cl₂, δ): 169.23, 167.64, 166.33, 161.76, 157.53, 157.20, 151.65, 151.28, 150.82, 149.28, 149.20, 147.21, 143.33, 143.13, 139.64, 138.55, 138.42, 138.11, 137.44, 131.78, 131.18, 130.64, 129.99, 129.47, 128.27, 128.20, 127.80, 125.35, 125.00, 124.87, 123.74, 123.18, 122.78, 121.31, 121.17, 120.29, 120.25, 106.28, 103.59, 68.96, 32.30, 29.98, 29.96, 29.78, 29.72, 29.62, 26.39, 23.08, 14.28; IR (solid): ν = 3047 (w), 2922 (w), 2853 (w), 1587 (m), 1541 (w), 1477 (m), 1441 (m), 1412 (m), 1400 (m), 1369 (w), 1298 (w), 1269 (w), 1229 (w), 1161 (s), 1061 (w), 1030 (w), 829 (s), 789 (s), 754 (s), 727 (s), 696 (s), 669 (s), 623 (m), 555 (m) cm⁻¹; MS (ESI, m/z): 1121.6 [M-PF₆]⁺ (calc. 1121.5); Anal. calcd. for C₆₄H₇₂F₆IrN₄O₂P·0.5H₂O (1275.47): C 60.27, H 5.77, N 4.39; found: C 60.32, H 5.52, N 4.23.

g) Preparation of 4. A yellow suspension of tetrakis(2-phenylpyridine-C,N)di(μ-chloro)diiridium(III) (75 mg, 0.0704 mmol, 1.00 eq.) and G1ppppy (177 mg, 0.141 mmol, 2.00 eq.) in MeOH (25 mL) and CH₂Cl₂ (25 mL) was refluxed under an inert atmosphere of N₂ in the dark for 15 h. The orange solution was then cooled down to room temperature and solid ammonium hexafluorophosphate (115 mg, 0.704 mmol, 10.0 eq.) was added to the solution. The mixture was stirred for 30 min at room temperature and then evaporated to dryness. The crude material was purified by column chromatography (Alox 90, CH₂Cl₂:hexane = 1:1 → CH₂Cl₂ → CH₂Cl₂:MeOH = 100:2) yielding the desired product as an orange solid (253 mg, 0.133 mmol, 96%). ¹H NMR (500 MHz, CD₂Cl₂, δ): 8.66–8.62 (m, J = 11.6 Hz, 2H), 8.19 (t, J = 7.9 Hz, 1H), 7.95 (d, J = 5.5 Hz, 1H), 7.92–7.86 (m, 3H), 7.80 (t, J = 7.8 Hz, 1H), 7.74 (d, J = 5.6 Hz, 1H), 7.69 (s, 1H), 7.64 (d, J = 5.9 Hz, 1H), 7.59 (d, J = 7.8 Hz, 1H), 7.45 (t, J = 6.6 Hz, 1H), 7.29 (d, J = 7.8 Hz, 1H), 7.14–7.07 (m, 4H), 7.01 (t, J = 7.5 Hz, 2H), 6.87 (t, J = 7.5 Hz, 1H), 6.84–6.78 (m, 3H), 6.69–6.57 (m, 7H), 6.47–6.42 (m, 3H), 6.01 (d, J = 7.7 Hz, 1H), 5.63 (d, J = 7.6 Hz, 1H), 5.11 (s, 4H), 3.97 (t, J = 6.5 Hz, 8H), 1.82–1.74 (m, 8H), 1.51–1.43 (m, 8H), 1.43–1.24 (s, 64H), 0.92 (t, J = 6.7 Hz, 12H); ¹³C NMR (126 MHz, CD₂Cl₂, δ): 169.23, 167.63, 166.35, 161.22, 161.02, 157.60, 157.19, 151.38, 151.27, 150.80, 149.31, 149.21, 147.18, 143.32, 143.12, 139.66, 139.12, 138.54, 138.41, 138.09, 137.85, 137.63, 131.79, 131.19, 130.64, 130.00, 129.49, 128.27, 128.18, 127.79, 125.46, 125.00, 124.87, 123.74, 123.20, 122.77, 121.37, 121.18, 120.28, 120.23, 107.01, 106.08, 104.50, 100.97, 70.76, 68.54, 32.32, 30.07, 30.04, 30.01, 29.99, 29.80, 29.75, 29.65, 26.42, 23.09, 14.28; IR (solid): ν = 2922 (w), 2853 (w), 1593 (m), 1543 (w), 1454 (w), 1371 (w), 1300 (w), 1269 (w), 1157 (m), 1057 (w), 831 (s), 787 (s), 754 (s), 729 (s), 694 (s), 621 (s) cm⁻¹; MS (ESI, m/z): 1758.4 [M-PF₆]⁺ (calc. 1758.0). Anal. calcd. for C₁₀₆H₁₄₀F₆IrN₄O₆P (1903.45): C 66.89, H 7.41, N 2.94; found: C 66.92, H 7.20, N 2.75.

Device preparation: PEDOT:PSS was purchased from HC-Starck and solvents used were obtained from Aldrich. ITO-coated glass plates (15 Ω □⁻¹) were patterned using conventional photolithography (obtained from Naranjosubstrates). The substrates were extensively cleaned using sonification in subsequently water-soap, water, and 2-propanol baths. After drying, the substrates were placed in a UV-ozone cleaner (Jelight 42-220) for 20 min.

The electroluminescent devices were prepared as follows. Transparent thin films of complexes 1–3 containing different amounts of the ionic liquid (1-butyl-3-methylimidazolium hexafluorophosphate) were obtained by spinning from acetonitrile solutions using concentrations of 20 mg mL⁻¹ at 2000 rpm for 40 s, resulting in 80-nm-thick films. Prior to the deposition of the emitting layer, a 100-nm layer of PEDOT:PSS was deposited to increase the device preparation yield. The thickness of the films was determined using an Ambios XP1 profilometer. After spinning the organic layers, the samples were transferred to an inert atmosphere glovebox (< 0.1 ppm O₂ and H₂O, MBraun) and dried on a hot plate at 80 °C for 1 h. Aluminum metal electrodes (80 nm) were thermally evaporated using a shadow mask

under a vacuum ($< 1 \times 10^{-6}$ mbar) using an Edwards Auto500 evaporator integrated into an inert atmosphere glovebox.

Current density and luminance versus voltage were measured using a Keithley 2400 source meter and a photodiode coupled to a Keithley 6485 pico-amperometer using a Minolta LS100 to calibrate the photocurrent. EQEs were determined using an integrated sphere coupled to an UDT instruments S370 Optometer. An Avantes luminance spectrometer was used to measure the EL spectrum. Lifetime data were obtained by applying a constant voltage over the device and monitoring the current flow and simultaneously the current generated by a Si-photodiode (Hamamatsu S1336-8BK) calibrated using a Minolta LS100 luminance meter. Custom-made equipment consisting of a multichannel rack, from muetta consult, 16 boards with power source, and DAQ (data acquisition)-12 bits ADC (analogue to digital converter) was used to measure the luminance and current density over the time. A custom-designed labview program was used to control the equipment and gather the data on a personal computer. Both the multi-channel rack and the PC are connected via an autonomic power supply unit (SALICRU SLC cube).

Computational Details: DFT calculations were carried out with the D.02 revision of the Gaussian 03 program package [47] using Becke's three-parameter B3LYP exchange-correlation functional [48–50] together with the 6-31G** basis set for C, H, N, and O atoms [51] and the "double- ζ " quality LANL2DZ basis set for the Ir element [52]. An effective core potential (ECP) replaces the inner core electrons of Ir leaving the outer core $[(5s)^2(5p)^6]$ electrons and the $(5d)^6$ valence electrons of Ir(III). The geometries of the singlet ground state (S_0) and of the triplet excited states (3T_1 and 3MC) were fully optimized. Triplet states were calculated at the spin-unrestricted UB3LYP level with a spin multiplicity of 3. The expected values calculated for S^2 were always smaller than 2.05.

Acknowledgements

This work has been supported by the European Union (CELLO, STRP 248043), ESF Eurocores-05SONS-FP-021, the Spanish Ministry of Science and Innovation (MICINN) (MAT2006-28185-E, MAT2007-61584, CSD2007-00010, and CTQ2006-14987-C02-02), the Generalitat Valenciana (ACOMP/2009/269), European FEDER funds, the Swiss National Science Foundation, and the Swiss National Center of Competence in Research "Nanoscale Science." R.D.C. acknowledges the support of a FPU grant of the MICINN. Jorge Ferrandós assistance with the lifetime setup is greatly appreciated.

Received: January 8, 2010
Published online: April 7, 2010

- [1] J. D. Slinker, J. Rivnay, J. S. Moskowitz, J. B. Parker, S. Bernhard, H. D. Abruña, G. G. Malliaras, *J. Mater. Chem.* **2007**, *17*, 2976.
- [2] Q. Pei, G. Yu, C. Zhang, Y. Yang, A. J. Heeger, *Science* **1995**, *269*, 1086.
- [3] P. Matyba, K. Maturova, M. Kemerink, N. D. Robinson, L. Edman, *Nat. Mater.* **2009**, *8*, 672.
- [4] J. C. deMello, N. Tessler, S. C. Graham, R. H. Friend, *Phys. Rev. B* **1998**, *57*, 12951.
- [5] J. D. Slinker, J. A. DeFranco, M. J. Jaquith, W. R. Silveira, Y. Zhong, J. M. Moran-Mirabal, H. G. Graighead, H. D. Abruña, J. A. Marohn, G. G. Malliaras, *Nat. Mater.* **2007**, *6*, 894.
- [6] J. C. deMello, *Phys. Rev. B* **2002**, *66*, 235210.
- [7] H. C. Su, C. C. Wu, F. C. Fang, K. T. Wong, *Appl. Phys. Lett.* **2006**, *89*, 261118.
- [8] H. C. Su, F. C. Fang, T. Y. Hwu, H. H. Hsieh, H. Chen, G. Lee, S. Peng, K. T. Wong, C. C. Wu, *Adv. Funct. Mater.* **2007**, *17*, 1019.
- [9] H. J. Bolink, E. Coronado, R. D. Costa, N. Lardiés, E. Ortí, *Inorg. Chem.* **2008**, *47*, 9149.
- [10] C. Rothe, C.-J. Chiang, V. Jankus, K. Abdullah, X. Zeng, R. Jitchati, A. S. Batsanov, M. R. Bryce, A. P. Monkman, *Adv. Funct. Mater.* **2009**, *19*, 2038.
- [11] F. De Angelis, S. Fantacci, N. Evans, C. Klein, S. M. Zakeeruddin, J. E. Moser, K. Kalyanasundaram, H. J. Bolink, M. Graetzel, M. K. Nazeeruddin, *Inorg. Chem.* **2007**, *46*, 5989.
- [12] H. C. Su, H. F. Chen, F. C. Fang, C. C. Liu, C. C. Wu, K. T. Wong, Y. H. Liu, S. M. Peng, *J. Am. Chem. Soc.* **2008**, *130*, 3413.
- [13] L. He, J. Qiao, L. Duan, G. Dong, D. Zhang, L. Wang, Y. Qiu, *Adv. Funct. Mater.* **2009**, *19*, 2950.
- [14] L. He, L. Duan, J. Qiao, R. Wang, P. Wei, L. Wang, Y. Qiu, *Adv. Funct. Mater.* **2008**, *18*, 2123.
- [15] A. B. Tamayo, S. Garon, T. Sajoto, P. I. Djurovich, I. M. Tsyba, R. Bau, M. E. Thompson, *Inorg. Chem.* **2005**, *44*, 8723.
- [16] J. D. Slinker, A. A. Gorodetsky, M. S. Lowry, J. Wang, S. Parker, R. Rohl, S. Bernhard, G. G. Malliaras, *J. Am. Chem. Soc.* **2004**, *126*, 2763.
- [17] R. D. Costa, E. Ortí, H. J. Bolink, S. Graber, S. Schaffner, M. Neuberger, C. E. Housecroft, E. C. Constable, *Adv. Funct. Mater.* **2009**, *19*, 3456.
- [18] R. D. Costa, F. J. Céspedes-Guirao, E. Ortí, H. J. Bolink, J. Gierschner, F. Fernández-Lázaro, A. Sastre-Santos, *Chem. Commun.* **2009**, 3886.
- [19] H. J. Bolink, E. Coronado, R. D. Costa, E. Ortí, M. Sessolo, S. Graber, K. Doyle, M. Neuberger, C. E. Housecroft, E. C. Constable, *Adv. Mater.* **2008**, *20*, 3910.
- [20] S. Graber, K. Doyle, M. Neuberger, C. E. Housecroft, E. C. Constable, R. D. Costa, E. Ortí, D. Repetto, H. J. Bolink, *J. Am. Chem. Soc.* **2008**, *130*, 14944.
- [21] R. D. Costa, E. Ortí, H. J. Bolink, S. Graber, C. E. Housecroft, M. Neuberger, S. Schaffner, E. C. Constable, *Chem. Commun.* **2009**, 2029.
- [22] G. G. Malliaras, J. C. Scott, *J. Appl. Phys.* **1998**, *83*, 5399.
- [23] H. J. Bolink, L. Cappelli, E. Coronado, M. Graetzel, M. Nazeeruddin, *J. Am. Chem. Soc.* **2006**, *128*, 46.
- [24] H. J. Bolink, L. Cappelli, E. Coronado, M. Graetzel, E. Ortí, R. D. Costa, M. Viruela, M. K. Nazeeruddin, *J. Am. Chem. Soc.* **2006**, *128*, 14786.
- [25] G. Kalyuzhny, M. Buda, J. McNeill, P. Barbara, A. J. Bard, *J. Am. Chem. Soc.* **2003**, *125*, 6272.
- [26] L. J. Soltzberg, J. Slinker, S. Flores-Torres, D. Bernards, G. G. Malliaras, H. D. Abruña, J. S. Kim, R. H. Friend, M. D. Kaplan, V. Goldberg, *J. Am. Chem. Soc.* **2006**, *128*, 7761.
- [27] J. D. Slinker, J.-S. Kim, S. Flores-Torres, J. H. Delcamp, H. D. Abruña, R. H. Friend, G. G. Malliaras, *J. Mater. Chem.* **2007**, *7*, 76.
- [28] G. W. V. Cave, C. L. Raston, *J. Chem. Educ.* **2005**, *82*, 468.
- [29] C. B. Smith, C. L. Raston, A. N. Sobolev, *Green Chem.* **2005**, *7*, 650.
- [30] G. W. V. Cave, C. L. Raston, *J. Chem. Soc. Perkin Trans. 1*, **2001**, 3258.
- [31] V. N. Kozhevnikov, A. C. Whitwood, D. W. Bruce, *Chem. Commun.* **2007**, 3826.
- [32] C. R. Schmid, C. A. Beck, J. S. Cronin, M. A. Staszak, *Org. Process Res. Dev.* **2004**, *8*, 670.
- [33] V. Prey, *Ber. Dtsch. Chem. Ges.* **1942**, *75*, 350.
- [34] H. J. Bolink, L. Cappelli, S. Cheylan, E. Coronado, R. D. Costa, N. Lardiés, M. K. Nazeeruddin, E. Ortí, *J. Mater. Chem.* **2007**, *17*, 5032.
- [35] M. S. Lowry, W. R. Hudson, R. A. Pascal, S. Bernhard, *J. Am. Chem. Soc.* **2004**, *126*, 14129.
- [36] M. G. Colombo, H. Güdel, *Inorg. Chem.* **1993**, *32*, 3081.
- [37] M. G. Colombo, A. Hauser, H. Güdel, *Inorg. Chem.* **1993**, *32*, 3088.
- [38] B. A. Hermann, L. J. Scherer, C. E. Housecroft, E. C. Constable, *Adv. Funct. Mater.* **2006**, *16*, 221.
- [39] E. C. Constable, V. Chaurin, C. E. Housecroft, M. Neuberger, S. Schaffner, *CrystEngComm* **2007**, *9*, 176.
- [40] D. W. Thompson, J. F. Wishart, B. S. Brunswig, N. Sutin, *J. Phys. Chem. A* **2001**, *105*, 8117.
- [41] F. Alary, J. L. Heully, L. Bijeire, P. Vicendo, *Inorg. Chem.* **2007**, *46*, 3154.
- [42] J. Van Houten, R. J. Watts, *J. Am. Chem. Soc.* **1976**, *98*, 4853.
- [43] S. T. Parker, J. Slinker, M. S. Lowry, M. P. Cox, S. Bernhard, G. G. Malliaras, *Chem. Mater.* **2005**, *17*, 3187.
- [44] E. S. Handy, A. J. Pal, M. F. Rubner, *J. Am. Chem. Soc.* **1999**, *121*, 3525.
- [45] D. R. Blasini, J. Rivnay, D. M. Smilgies, J. D. Slinker, S. Flores-Torres, H. D. Abruña, G. G. Malliaras, *J. Mater. Chem.* **2007**, *17*, 1458.

- [46] M. K. Nazeeruddin, R. T. Wegh, Z. Zhou, C. Klein, Q. Wang, F. De Angelis, S. Fantacci, M. Graetzel, *Inorg. Chem.* **2006**, *45*, 9245.
- [47] M. J. Frisch, G. W. Trucks, H. B. Schlegel, G. E. Scuseria, M. A. Robb, J. R. Cheeseman, J. A. Montgomery, Jr, T. Vreven, K. N. Kudin, J. C. Burant, J. M. Millam, S. S. Iyengar, J. Tomasi, V. Barone, B. Mennucci, M. Cossi, G. Scalmani, N. Rega, G. A. Petersson, H. Nakatsuji, M. Hada, M. Ehara, K. Toyota, R. Fukuda, J. Hasegawa, M. Ishida, T. Nakajima, Y. Honda, O. Kitao, H. Nakai, M. Klene, X. Li, J. E. Knox, H. P. Hratchian, J. B. Cross, V. Bakken, C. Adamo, J. Jaramillo, R. Gomperts, R. E. Stratmann, O. Yazyev, A. J. Austin, R. Cammi, C. Pomelli, J. W. Ochterski, P. Y. Ayala, K. Morokuma, G. A. Voth, P. Salvador, J. J. Dannenberg, V. G. Zakrzewski, S. Dapprich, A. D. Daniels, M. C. Strain, O. Farkas, D. K. Malick, A. D. Rabuck, K. Raghavachari, J. B. Foresman, J. V. Ortiz, Q. Cui, A. G. Baboul, S. Clifford, J. Cioslowski, B. B. Stefanov, G. Liu, A. Liashenko, P. Piskorz, I. Komaromi, R. L. Martin, D. J. Fox, T. Keith, M. A. Al-Laham, C. Y. Peng, A. Nanayakkara, M. Challacombe, P. M. W. Gill, B. Johnson, W. Chen, M. W. Wong, C. Gonzalez, J. A. Pople, *Gaussian 03*, Revision D.02, Gaussian, Inc., Wallingford CT, **2004**.
- [48] A. D. Becke, *J. Chem. Phys.* **1988**, *88*, 2547.
- [49] A. D. Becke, *Phys. Rev. A* **1988**, *38*, 3098.
- [50] A. D. Becke, *J. Chem. Phys.* **1993**, *98*, 5648.
- [51] M. M. Francl, W. J. Pietro, W. J. Hehre, J. S. Binkley, M. S. Gordon, D. J. Defrees, J. A. Pople, *J. Chem. Phys.* **1982**, *77*, 3654.
- [52] P. J. Hay, W. R. Wadt, *J. Chem. Phys.* **1985**, *82*, 299.